

# A JOINT SOURCE CHANNEL ARITHMETIC MAP DECODER USING PROBABILISTIC RELATIONS AMONG INTRA MODES IN PREDICTIVE VIDEO COMPRESSION

Hossein Kourkchi, Student Member, IEEE, William E. Lynch, Member, IEEE, and M. Omair Ahmad, Fellow, IEEE

Department of Electrical and Computer Engineering, Concordia University  
1455 de Maisonneuve Blvd. W., Montréal, Québec, Canada H3G 1M8  
Email: {h\_kourkc, blynch, omair}@ece.concordia.ca

## ABSTRACT

In this paper, residual redundancy in compressed videos is exploited to alleviate transmission errors using joint source channel arithmetic decoding. A new method is proposed to estimate *a priori* probability in MAP metric of H.264 *intra* modes decoder. The decoder generates a decoding tree using a breadth first search algorithm. An introduced statistical model is then implemented stage by stage over the decoding tree. In this model, *a priori* PMF of *intra* block modes in a macroblock is estimated from the *intra* block modes seated in its spatially adjacent macroblocks previously generated up to the current stage of the decoding tree. The estimated PMFs are categorized as either reliable or unreliable based on their local entropies. In the unreliable case, the decoder assumes uniform PMF and switch to ML metric instead. The simulation results show the proposed method reduces the error rate 1% to 13% at various SNRs compared to the ML.

**Index Terms**— Joint source-channel arithmetic coding, maximum a posteriori (MAP), H.264, *intra* modes

## 1. INTRODUCTION

In compression standards, *e.g.*, H.264 and high efficiency video compression (HEVC), arithmetic coding (AC) has been employed as source coding to exploit and remove redundancy. However, in practice, some residual redundancy remains in the output. This could be a result of either mismatch between the statistical models used in the encoder and the actual statistics of the encoder input, or a constraint on the latency and complexity of the encoder [1].

In joint source channel arithmetic coding (JSCAC), the decoder uses the residual redundancy along with intentionally added redundancy [2] to enhance the error resilience [3].

In [4]-[6], a maximum *a posteriori* (MAP) decoder exploits the redundancy by modeling the source encoder output using a Markov process, without considering the semantic and syntactic information of the encoder input, and

in turn, the decoder output.

In [7], the correlation between motion vectors of H.264 is modeled using a first-order Markov process. The parameters of the statistical model are calculated at the encoder and transmitted as side information to the decoder through an error-free channel. However, this error-free transmission imposes an overhead on the system.

In [8], the syntax elements (SE) of H.264 are statistically modeled. The decoder divides the input bit sequence into variable length bit sequences (input codewords), each of which is decoded to an SE using the variable length code (VLC) [9]. At each stage, it generates all possible codeword candidates and their decoding metric and finally it keeps only the candidate maximizing the decoding metric. There are three problems with this method. First, errors in a codeword may result in syntactic errors in future codewords but not in the current codeword. Second, the statistical model may not always be reliable for all conditions, *e.g.*, non-stationary processes [10], and may mislead the decoder. Third, codeword-by-codeword decoding is not applicable for AC.

In this paper, a sequential MAP decoder is proposed that utilizes a breadth-first algorithm (M-algorithm (MA) [11]) for constructing a decoding tree. The decoding tree is constructed channel bit by channel bit and the decoding metric is calculated in each stage for the candidates based on decoder input and the *a priori* information exploited from the interdependencies in previously decoded SEs. The *intra* modes are addressed as highly correlated SEs. The *intra* mode probability mass function (PMF) is calculated from previously decoded *intra* modes. When the previously decoded *intra* modes are too diverse, the calculated PMF is deemed unreliable for the current SE. The entropy of the *intra* modes of previously decoded *intra* blocks is used as the diversity measure. In the unreliable cases, the decoder neglects the *a priori* probabilities estimated. The simulation results show 1% to 13% PER reduction compared to the maximum likelihood (ML) decoding.

In Section 2, the structure of joint source channel coding and the MAP decoding is briefly explained. The proposed MAP decoding using *intra* mode statistic estimation is proposed in Section 3. Simulation and results are provided in

This work was supported by the Natural Sciences and Engineering Research Council (NSERC) of Canada, the Centre for Advanced Systems and Technologies in Communications (SYTACom), and the Regroupement Stratégique en Microélectronique du Québec (ReSMiQ).

Section 4 followed by Section 5 that concludes the work.

## 2. MAP DECODING OF JSCAC

Since binary AC removes the redundancy in SEs efficiently, it is fragile in noisy transmissions. To cope with the noise, JSCAC assigns a forbidden symbol (FS) to symbol alphabet, which is never encoded [2]. Observing the FS at the receiver helps the decoder to detect and correct errors.

In video coding standards, the outcome of the predictive process is a stream of SEs such as coefficient levels, motion vectors, and *intra* modes [9]. A binarizer maps the sequence of SEs  $\mathbf{x}$  to a sequence of binary symbols (bins)  $\mathbf{s}$ , where  $s_i$  is either 0 or 1. The binary arithmetic coder with FS compresses  $\mathbf{s}$  to a bit sequence  $\mathbf{u}$  of length  $\ell_u$ , where  $u_i$  is either bit 0 or 1. The bit sequence  $\mathbf{u}$  after modulation goes to a communication channel, modeled by the addition of white Gaussian noise (AWGN),  $\mathbf{n}$ , and its output is  $\mathbf{y}$ .

The MAP decoder estimates  $\mathbf{u}$ ,  $\mathbf{s}$  and  $\mathbf{x}$ , represented, respectively, by  $\hat{\mathbf{u}}$ ,  $\hat{\mathbf{s}}$  and  $\hat{\mathbf{x}}$  in a way that maximize the *a posteriori* probability as

$$\hat{\mathbf{u}} = \arg \max_{\tilde{\mathbf{u}} \in \mathcal{B}} P(\tilde{\mathbf{u}}|\mathbf{y}) = \arg \max_{\tilde{\mathbf{u}} \in \mathcal{B}} \frac{P(\tilde{\mathbf{u}})P(\mathbf{y}|\tilde{\mathbf{u}})}{P(\mathbf{y})}, \quad (1)$$

where  $\mathcal{B}$  is the set of all possible bit sequences. Since the cardinality of  $\mathcal{B}$  is very large, it is infeasible to calculate all of the *a posteriori* probabilities.

To moderate the complexity a breadth-first suboptimal sequential decoding method, MA [11], is used. Using a decoding tree, the decoder generates bit sequence candidates  $\tilde{\mathbf{u}}^j$ , of length  $j$ , recursively by extending previous candidates in stage  $j-1$ . At each stage, it keeps only the best  $M$  candidates based on their metric. By applying logarithm to Equation (1) and noting that the channel is memoryless, the decoding metric for the candidate  $\tilde{\mathbf{u}}^j$  is given by

$$m_{\tilde{\mathbf{u}}^j} = \log P(\mathbf{x}_{\tilde{\mathbf{u}}^j}) + \sum_{k=1}^j \log P(y_k|\tilde{u}_k) - \sum_{k=1}^j \log P(y_k) \quad (2)$$

where  $\mathbf{x}_{\tilde{\mathbf{u}}^j}$  is the SE sequence corresponding to  $\tilde{\mathbf{u}}^j$ . The last term is identical for all  $\tilde{\mathbf{u}}^j$ s, and hence, it can be discarded. The middle term is dependent on the channel transition probability. The first term,  $\log P(\mathbf{x}_{\tilde{\mathbf{u}}^j})$ , is the *a priori* probability of the SE sequence. Two approaches are possible to deal with *a priori* probability. The first one is to use the simplifying assumption that all the SE sequences are equiprobable which converts the MAP to an ML decoder. The second approach is to estimate the *a priori* probability using the interdependencies between the SEs.

The block diagram of the proposed MAP decoder is shown in Fig. 1. The demodulation and candidate generator (DCG) generates the bit sequence candidates  $\tilde{\mathbf{u}}^j$  and, in turn, the corresponding bin sequences  $\mathbf{s}_{\tilde{\mathbf{u}}^j}$  and SE sequences  $\mathbf{x}_{\tilde{\mathbf{u}}^j}$ . The symbol checker discards the candidates that produce a FS. The syntax checker eliminates the candidates that violate the syntax or semantics of the H.264 standard. The *a priori* probability estimator calculates the probability of  $\mathbf{x}_{\tilde{\mathbf{u}}^j}$  and

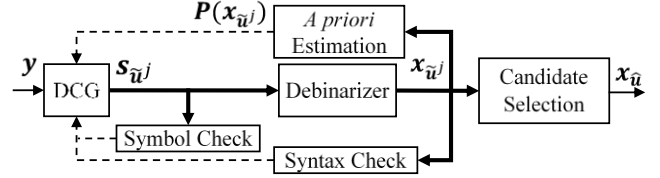


Fig. 1. Block diagram of the MAP decoder.

feeds it back into DCG to update the decoding metric of the candidate. Finally, the decoder emits the SE sequence  $\hat{\mathbf{x}}$  whose corresponding decoding metric  $m_{\hat{\mathbf{x}}}$  is the highest among all generated candidates.

One of the challenges in the metric calculation is different lengths of the generated SE sequences  $\mathbf{x}_{\tilde{\mathbf{u}}^j}$ 's for different realizations  $\tilde{\mathbf{u}}^j$ 's. Since the probability of an SE sequence realization generally decreases with the growth of its length, the maximization process should take the same number of SEs into consideration. The minimum length of  $\mathbf{x}_{\tilde{\mathbf{u}}^j}$ 's is  $\ell_j$ . By considering the first  $\ell_j$  SEs of  $\mathbf{x}_{\tilde{\mathbf{u}}^j}$ , a truncated sequence is constructed which is named  $\bar{\mathbf{x}}_{\tilde{\mathbf{u}}^j}$ . In (2),  $P(\mathbf{x}_{\tilde{\mathbf{u}}^j})$  is replaced by  $P(\bar{\mathbf{x}}_{\tilde{\mathbf{u}}^j})$ , and for the sake of simplifying the notation,  $\bar{\mathbf{x}}_{\tilde{\mathbf{u}}^j}$  is replaced by  $\bar{\mathbf{x}}$ . The term  $\log(P(\bar{\mathbf{x}}))$  is expanded by applying the chain rule in [10] as

$$\log(P(\bar{\mathbf{x}})) = \log(P(\bar{x}_1)) + \sum_{n=2}^{\ell_j} \log(P(\bar{x}_n|\bar{\mathbf{x}}^{n-1})), \quad (3)$$

where  $\bar{\mathbf{x}}^{n-1}$  is the first  $n-1$  elements of  $\bar{\mathbf{x}}$  and  $\bar{x}_n$  is the  $n^{\text{th}}$  element of  $\bar{\mathbf{x}}$ . By assuming that there is interdependency only among the spatially adjacent SEs,  $P(\bar{x}_n|\bar{\mathbf{x}}^{n-1})$  is

$$P(\bar{x}_n|\bar{\mathbf{x}}^{n-1}) = P(\bar{x}_n|\llbracket \bar{\mathbf{x}}^{n-1} \rrbracket), \quad (4)$$

where  $\llbracket \bar{\mathbf{x}}^{n-1} \rrbracket$  is the subset of  $\bar{\mathbf{x}}^{n-1}$  whose elements are spatially adjacent with the SE  $\bar{x}_n$ .  $\llbracket \bar{\mathbf{x}}^{n-1} \rrbracket$  is a sequence of the SEs that are previously decoded and spatially adjacent to the current SE  $\bar{x}_n$  which will be followed up in Section 3.1.

## 3. INTRA MODES MAP DECODER

In H.264 every frame is divided into  $16 \times 16$  macroblocks (MBs). In *intra* coding, prediction of the current MB is based on the previously coded data from the current frame [9]. Each MB is partitioned into either sixteen  $4 \times 4$  *intra* blocks or four  $8 \times 8$  *intra* blocks or is left as one  $16 \times 16$  *intra* block. In the  $4 \times 4$  and  $8 \times 8$  cases, there are 9 possible directional *intra* modes as shown in Fig. 2 (a).  $l_m$  is the *intra* mode index corresponding to *intra* mode  $m$ . The *intra* mode indices are in angular order.

### 3.1. Adaptive intra mode PMF estimation

The decoder generates MBs of a frame row by row. The SEs in the three adjacent MBs ( $MB_{adj}$ ) at the top, left and up-left side of the current MB ( $MB_x$ ) are considered as spatially adjacent to the SEs in the current MB as shown in Fig. 2 (b). Here, a method is proposed to estimate the distribution of *intra* modes in the current MB ( $MB_x$ ) from the decoded neighboring MBs ( $MB_{adj}$ ), i.e.,  $P(\bar{x}_n|\llbracket \bar{\mathbf{x}}^{n-1} \rrbracket)$  in (4).

To calculate the PMF of *intra* block modes in  $MB_x$  as

accurately as possible, a conditional probability that relates the *intra* block mode patterns in  $MB_{adj}$  and  $MB_x$  *intra* blocks should be used. The number of possible patterns for *intra* modes in  $MB_{adj}$  is a large number. For example, if  $MB_{adj}$  consists of  $4 \times 4$  *intra* blocks, the number of possibilities is equal to  $9^{3 \times 16} \cong 6.3 \times 10^{45}$ . The large number of possibilities makes precalculation of the conditional probabilities infeasible.

To moderate this complexity and also to statistically use a Markov information source model, instead of considering all possible patterns in  $MB_{adj}$ , only the distribution of *intra* modes in  $MB_{adj}$  is taken into account. The relation between PMF of *intra* modes in  $MB_x$  and PMF of *intra* modes in  $MB_{adj}$  is modeled by a transition conditional probability function  $P(M_b = m | M_{b'} = m')$ , where,  $b$  and  $b'$  are *intra* blocks in  $MB_x$  and  $MB_{adj}$ , respectively, and  $M_b$  and  $M_{b'}$  are their *intra* modes.  $MB_{adj}$  is modeled as an information source which emits *intra* modes with a certain PMF, and the *intra* modes in  $MB_x$  are their deviated versions. This deviation is modeled by this transition probability function.

To emit an *intra* mode by  $MB_{adj}$ , an *intra* block in  $MB_{adj}$  should be selected in random. Thus, the *intra* mode probability is estimated adaptively by normalizing the local histogram as

$$\hat{P}(M_{b'} = m') = \frac{\text{hist}(m', MB_{adj})}{\sum_{\tilde{m}} \text{hist}(\tilde{m}, MB_{adj})}, \quad b' \in MB_x, \quad (5)$$

where  $m'$  and  $\tilde{m}$  are *intra* modes, and function  $\text{hist}(m, MB_{adj})$  counts the number of blocks in  $MB_{adj}$  whose *intra* modes is equal to  $m$ . Using the total probability rule [10], the PMF estimation of *intra* modes in the current MB is written as

$$\hat{P}(M_b = m) = \sum_{m'} \hat{P}(M_{b'} = m') P(M_b = m | M_{b'} = m'). \quad (6)$$

Since  $\hat{P}(M_b = m)$  is calculated adaptively, this type of decoder is called *MAP-Ad* decoder.

### 3.2. Transition probability calculation

*Intra* modes are usually chosen by the encoder based on a rate-distortion optimization mechanism [12], and they are aligned to the image texture of MBs. In natural images, the texture varies gradually in adjacent MBs. Thus, directional *intra* modes of the current MB and its neighbors are highly correlated [13], *i.e.*, if a directional mode is highly probable in the neighboring MBs, that mode and the modes close to it in an angular sense (see Fig. 2(a)) are highly probable in the current MB. In order to work with the *intra* modes ( $m$ ) in the angular order conveniently, their indexes ( $i_m$ ) are used. *Intra* mode index of randomly chosen *intra* blocks  $b \in MB_x$  and  $b' \in MB_{adj}$  are random variables, respectively, denoted by  $I$  and  $I'$ .

When the neighboring mode is DC, there is no directional information in the adjacent MBs, and in turn, the PMF of *intra* modes in current MB is assumed to be uniform,

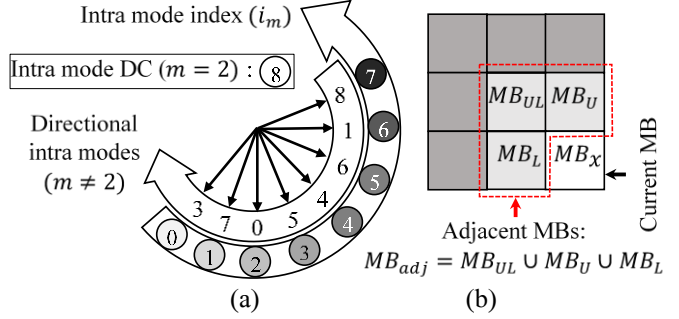


**Fig. 2.** (a) Intra prediction modes and their index  
(b) Spatially adjacent MBs to the current MB.

*i.e.*,  $P(I = i | I' = 8; 0 \leq i \leq 8) = 1/9$ . Similarly, the directional modes do not induce information in the DC mode, which results in  $P(I = 8 | 0 \leq I' \leq 7) = 1/9$ . To calculate the transition probability between two directional modes, the angular difference function is defined as

$$\Delta(I, I') = \begin{cases} |I - I'| & : 0 \leq |I - I'| \leq 4 \\ 8 - |I - I'| & : 4 < |I - I'| \leq 7, \end{cases} \quad (7)$$

Given that  $I$  and  $I'$  are two random variables,  $\Delta(I, I')$  output is a random variable denoted by  $\Omega$  with the range of 0 to 4.

To measure PMF of  $\Omega$  for typical videos, various natural raw videos from database [14] (~11000 frames) in QCIF format are *intra* encoded using H.264 reference software [15] with the QP value 28. PMF of  $\Omega$  is estimated as the normalized histogram of the angular difference, which is shown in Table 1. If  $\Omega = 4$ , the two directional modes in the current and the adjacent MBs are orthogonal, which is least probable, and when  $\Omega = 0$ , the two directional modes are in the same direction which is the most probable as expected.

**Table 1.** PMF of angular *intra* mode index difference

$\omega$	0	1	2	3	4
$P(\Omega = \omega)$	0.318	0.243	0.175	0.196	0.068

The transition probability for directional modes is written as  $P(I = i | I' = i'; 0 \leq i' \leq 7, 0 \leq i \leq 7) =$

$$= \begin{cases} \frac{1}{2} \times \frac{8}{9} P(\Omega = \Delta(i, i')) & : 1 \leq \Delta(i, i') \leq 3 \\ \frac{8}{9} P(\Omega = \Delta(i, i')) & : \Delta(i, i') = 0 \text{ or } 4. \end{cases} \quad (8)$$

When the angular difference is 1, 2 or 3, the *intra* mode index could alter either clockwise or counter-clockwise with equal probability, which is indicated by  $\frac{1}{2}$  coefficient. The  $\frac{8}{9}$  value is the probability  $P(I \neq 8 | 0 \leq I' \leq 7) = 1 - \frac{1}{9} = \frac{8}{9}$ .

### 3.3. Adjusting the MAP decoder

The *intra* mode PMF estimation might be unreliable, resulting in an increase in error rates. Here, a method is proposed to categorize MBs into two types, namely reliable MBs and unreliable MBs. The *intra* modes of each MB is a source of information whose output is a discrete random variable with PMF calculated in Section 3.1. The reliability categorization is done using the normalized entropy [16] of

this information source as

$$\bar{H}_{MB_x} = \frac{H_{MB_x} - H_{min}}{H_{max} - H_{min}}, \quad (9)$$

where  $H_{MB_x}$  is entropy of *intra* mode of  $MB_x$ , and  $H_{max}$  and  $H_{min}$  are maximum and minimum of the entropy of the source. In the proposed method, if  $\bar{H}_{MB_x}$  is greater than a predefined threshold,  $th\%$ , the MB is categorized as unreliable, and the decoder uses uniform *intra* mode PMF in the decoding metric. The procedure of setting the threshold is explained in Section 4. This method is called *MAP-Ad-Entp*.

#### 4. SIMULATION AND RESULTS

To find a proper entropy threshold, *i.e.*,  $th\%$ , video streams in database [14] are *intra* encoded using H.264 reference software [15] with quantization parameter (QP) 28 and passed through channel with SNR 5.2080 dB. The percentage of decoded frames that have packet error rates (PER) greater than the PER of the ML decoder is called the *corruption ratio* which is shown in Table 2 for various thresholds. In this Table average PER improvement over ML decoder is also provided. There is a trade-off between *corruption ratio* and improvement percentage. By decreasing the threshold the corruption ratio gets better, although performance of the system gets closer to ML algorithm on average. Based on this table, the threshold 37.5% is chosen, because in this threshold the proposed method not only outperforms the PER, but also it has a reasonable corruption ratio comparing to the *MAP-Ad* method ( $th=100\%$ ).

**Table 2.** Average PER improvement over ML decoder and corruption ratio for various thresholds in *MAP-Ad-Entp*

th%	12.50%	25%	37.50%	50%	62.50%	75%	87.50%	100%
PER Improvement %	1.37%	8.90%	13.01%	25.34%	33.56%	36.99%	32.88%	31.51%
Corruption Ratio %	2.97%	5.42%	7.34%	8.90%	9.83%	10.55%	12.09%	13.93%

In the simulations 300 frames of the videos *foreman*, *football*, *car-phone*, *table-tennis*, and *crew* [14] in QCIF format, 30 FPS, are used. The results are extendable to higher resolution videos, since similarity in adjacent MBs increases. All frames are considered as one slice and *intra* encoded with the QP value 28. The tests are done for FS probability  $10^{-3}$ . The SNR of the channel is in the range 7.335 dB, 6.7895 dB, 5.208 dB and 4.3232 dB. The value of M for MA is set to 16 for all simulations. The simulations run on a personal computer with a 2.8GHz processor, until at least 60 erroneous packets are decoded.

PER is calculated separately by simulation for the mentioned videos for the methods ML, *MAP-Ad* and *MAP-Ad-Entp-37%*. The results for different SNRs are represented in Table 3. As expected *MAP-Ad-Entp* has better performance than ML in terms of all error rates. Albeit moderate, this improvement can be enhanced by an iterative mechanism similar to [17]. It can be seen in this table, *MAP-Ad-Entp* has better performance for almost all videos, while *MAP-Ad* works well just for some particular videos, because *MAP-Ad-Entp* avoids unreliable *a priori* information by thresholding mechanism on local entropies.

Videos with high spatial activities, *e.g.*, *football*, have more unreliable MBs. As expected in such cases, MAP has higher error rates than ML, because *intra* mode estimation misleads the decoder, while the performance of *MAP-Ad-Entp* is improved or it is not noticeably changed with respect to ML performance. These results justify the efficiency of the *a priori* modeling of *intra* modes, and also the efficiency of the mechanism of entropy thresholding in the *MAP-Ad-Entp* method.

The cost of PER reduction by MAP decoders is growth of the computational complexity. As expected this cost in *MAP-Ad-Entp* is lower than *MAP-Ad*, because *MAP-Ad-Entp* saves some calculations of *a priori* probabilities in unreliable MBs, while *MAP-Ad* decoder calculates *a priori* probability of all MBs. The efficiency of *MAP-Ad-Entp* method in terms of error rates and computational complexity is borne out by these results.

**Table 3.** PER and average running time per packet *MAP-Ad*, *MAP-Ad-Entp-37.5%* and ML decoders in various channel SNRs and different videos

Video	Method	Channel SNR				T(sec)
		4.32 dB	5.2 dB	6.78 dB	7.34 dB	
Foreman	ML	9.94E-01	7.76E-01	2.36E-02	3.62E-03	1.258
	MAP-Ad-Entp-37.5%	9.90E-01	7.34E-01	2.05E-02	3.51E-03	2.07
	MAP-Ad	9.54E-01	5.77E-01	1.23E-02	2.41E-03	2.62
Car-phone	ML	9.91E-01	7.41E-01	2.21E-02	3.41E-03	1.183
	MAP-Ad-Entp-37.5%	9.74E-01	6.15E-01	1.50E-02	2.70E-03	2.153
	MAP-Ad	9.55E-01	5.45E-01	1.05E-02	1.97E-03	2.7
Crew	ML	9.90E-01	7.37E-01	2.35E-02	3.39E-03	1.233
	MAP-Ad-Entp-37.5%	9.77E-01	6.95E-01	2.10E-02	3.13E-03	2.05
	MAP-Ad	9.63E-01	6.83E-01	2.41E-02	3.39E-03	2.588
Table-tennis	ML	9.90E-01	7.23E-01	2.00E-02	3.04E-03	1.103
	MAP-Ad-Entp-37.5%	9.85E-01	6.86E-01	1.77E-02	2.75E-03	1.855
	MAP-Ad	9.91E-01	7.41E-01	2.19E-02	2.92E-03	2.49
Football	ML	9.86E-01	7.45E-01	1.94E-02	2.94E-03	1.308
	MAP-Ad-Entp-37.5%	9.78E-01	7.37E-01	1.98E-02	2.94E-03	2.205
	MAP-Ad	9.64E-01	7.70E-01	3.54E-02	4.51E-03	2.825
Average	ML	9.90E-01	7.45E-01	2.17E-02	3.28E-03	1.216
	MAP-Ad-Entp-37.5%	9.81E-01	6.93E-01	1.88E-02	3.01E-03	2.066
	MAP-Ad	9.65E-01	6.63E-01	2.08E-02	3.04E-03	2.644

#### 5. CONCLUSION

In this paper, a new statistical model has been proposed to estimate *a priori* probabilities in MAP metric to exploit residual redundancy in H.264. In [8] data stream is decoded codeword-by-codeword using VLC, while in the proposed decoder generates the candidates bit by bit using JSCAC. In the introduced method the PMF of *intra* modes in a MB is estimated adaptively using the SEs located in the spatially adjacent to MBs generated earlier in the decoding tree. In the new method, the estimation is categorized as either reliable or unreliable based on the local entropy of *intra* modes in adjacent MBs, and the decoder switches adaptively to ML in unreliable cases. The simulation results show improvement in PER comparing to ML decoder. In future work, by designing more sophisticated *a priori* probability estimator and MB reliability detector error correction could be improved.

## 6. REFERENCES

- [1] T. Guionnet and C. Guillemot, "Soft and joint source-channel decoding of quasi-arithmetic codes," *EURASIP Journal on Applied Signal Processing*, vol. 2004, pp. 393-411, 2004.
- [2] M. Grangetto, P. Cosman and G. Olmo, "Joint source/channel coding and MAP decoding of arithmetic codes," *IEEE Transactions on Communications*, vol. 53, no. 6, pp. 1007-1016, June 2005.
- [3] H. Kourkchi, W. E. Lynch and M. O. Ahmad, "Improving MAP arithmetic decoding of H.264 intra modes using residual redundancy," in *Proceedings of International Conference on Digital Image Processing*, Los Angeles, USA, April 2015.
- [4] N. Phamdo and N. Farvardin, "Optimal detection of discrete Markov sources over discrete memoryless channels—Applications to combined-source channel coding," *IEEE Transaction in Information Theory*, vol. 40, p. 186–193, 1994.
- [5] D. J. Miller and M. Park, "A sequence-based approximate mmse decoder for source coding over noisy channels using discrete hidden markov models," *IEEE Transactions on Communications*, vol. 46, no. 2, pp. 222-231, Feb 1998.
- [6] F. Lahouti and A. K. Khandani, "Efficient source decoding over memoryless noisy channels using higher order Markov models," *IEEE Transactions on Information Theory*, vol. 50, no. 9, pp. 2103-2118, September 2004.
- [7] A. H. Murad and T. E. Fuja, "Exploiting the residual redundancy in motion estimation vectors to improve the quality of compressed video transmitted over noisy channels," in *Proceedings International Conference on Image Processing*, Chicago, IL, 1998.
- [8] F. Caron and S. Coulombe, "Video error correction using soft-output and hard-output maximum likelihood decoding applied to an H.264 baseline profile," *IEEE Transactions on Circuits and Systems for Video Technology*, vol. 7, no. 25, pp. 1161-1174, July 2015.
- [9] I. E. Richardson, *The H.264 Advanced Video Compression Standard*, 2nd Edition, John Wiley, 2010.
- [10] A. Papoulis and S. U. Pillai, *Probability, random variables, and stochastic processes*, Boston: McGraw-Hill, 2002.
- [11] J. B. Anderson and S. Mohan, *Source and Channel Coding: An Algorithmic Approach*, Norwell, MA: Kluwer Academic Publisher, 1991.
- [12] S. Milani, "Fast H.264/AVC FRExt intra coding using belief propagation," *IEEE Transactions on Image Processing*, vol. 20, no. 1, pp. 121-131, Jan. 2011.
- [13] L. Z. B. Luo, "Fast intra-prediction mode selection method for H.264 video coding," in *International conference on intelligent system design and engineering application*, Changsha, 2010.
- [14] <http://trace.eas.asu.edu/yuv/index.html>.
- [15] "H.264/AVC Software Coordination JM Software," [Online]. Available: <http://iphome.hhi.de/suehring/tml/>.
- [16] T. M. Cover and J. A. Thomas, *Elements of information theory*, Hoboken, N.J. : Wiley-Interscience, 2nd ed, 2006.
- [17] S. Ben Jamaa, M. Kieffer and P. Duhamel, "Improved sequential MAP estimation of CABAC encoded data with objective adjustment of the complexity/efficiency tradeoff," *IEEE Transactions on Communications*, vol. 57, no. 7, pp. 2014-2023, July 2009.